

# Incorporation of Linear Spacer Molecules in Vapor-Deposited Silicone Polymer Thin Films

Anil Kumar H. Achyuta,<sup>†</sup> Aleksandr J. White,<sup>‡</sup> Hilton G. Pryce Lewis,<sup>‡</sup> and Shashi K. Murthy<sup>\*†</sup>

Department of Chemical Engineering, Northeastern University, Boston, Massachusetts 02115, and GVD Corporation, Cambridge, Massachusetts 02138

Received October 15, 2008; Revised Manuscript Received January 19, 2009

**ABSTRACT:** Poly(trivinyltrimethylcyclotrisiloxane) or polyV<sub>3</sub>D<sub>3</sub> is a promising insulating thin film known for its potential application in neural probe fabrication. However, its time-consuming synthesis rate renders it impractical by manufacturing standards. Previously, the growth mechanism of polyV<sub>3</sub>D<sub>3</sub> was shown to be affected by significant steric barriers. This article describes the synthesis of a copolymer of polyV<sub>3</sub>D<sub>3</sub> via initiated chemical vapor deposition (iCVD) using V<sub>3</sub>D<sub>3</sub> as the monomer, hexavinylidisiloxane (HVDS) as a spacer, and *tert*-butyl peroxide (TBP) as the initiator to obtain nearly a 4-fold increase in deposition rate. The film formation kinetics is limited by the adsorption of the reactive species on the surface of the substrate with an activation energy of  $-41.5$  kJ/mol with respect to substrate temperature. The films deposited are insoluble in polar and nonpolar solvents due to their extremely cross-linked structure. They have excellent adhesion to silicon substrates, and their adhesion properties are retained after soaking in a variety of solvents. Spectroscopic evidence shows that the films do not vary in structure after boiling in DI water for 1 h, illustrating hydrolytic stability. PolyV<sub>3</sub>D<sub>3</sub>–HVDS has a bulk resistivity of  $(5.6 \pm 1) \times 10^{14} \Omega \cdot \text{cm}$ , which is comparable to that of parylene-C, the insulating thin film currently used in neuroprosthetic devices.

## Introduction

Poly(trivinyltrimethylcyclotrisiloxane) (polyV<sub>3</sub>D<sub>3</sub>) thin films synthesized by initiated chemical vapor deposition (iCVD) are flexible and hydrolytically stable and have good insulation properties to serve as insulating coatings on neuroprosthetic devices.<sup>1</sup> This material adheres well to silicon substrates and is insoluble in polar and nonpolar solvents due to its highly cross-linked nature. Additionally, polyV<sub>3</sub>D<sub>3</sub> coatings on silicon wafer substrates possess high bulk resistivity and have resisted dielectric breakdown in a direct current (dc) biased saline soak for several years.<sup>2</sup> Also, this material has very low surface roughness that may facilitate diminished tissue reaction in the brain when implanted along with the device. The iCVD polymerization of polyV<sub>3</sub>D<sub>3</sub> is governed by a surface growth mechanism, which is best suited for coating high-aspect-ratio neural probes which have micron-scale features.

Previous work by O'Shaughnessy et al.<sup>1</sup> has shown that polyV<sub>3</sub>D<sub>3</sub> can be synthesized by iCVD using V<sub>3</sub>D<sub>3</sub> as the monomer and *tert*-butyl peroxide (TBP) as the initiator. The reaction occurs through the addition of activated peroxide radicals to the vinyl moieties present in the side chains of V<sub>3</sub>D<sub>3</sub> monomer. The addition of activated radicals is followed by propagation along the side chains, resulting in a hydrocarbon backbone with cyclic siloxane pendant groups. The involvement of each monomer unit in three separate chains results in a dense network of cross-linked polymer having a high molecular weight. However, the involvement of each V<sub>3</sub>D<sub>3</sub> monomer unit during chain growth in multiple polymer chains offers significant steric hindrance for chain mobility during the propagation step in the polymerization reaction. This steric barrier is present because the activated V<sub>3</sub>D<sub>3</sub> monomer units require aligning in certain conformations to interact with other large V<sub>3</sub>D<sub>3</sub> monomer units, resulting in a slow film deposition rate. Furthermore, the V<sub>3</sub>D<sub>3</sub> polymerization reaction through iCVD is surface reaction-

limited, and such reactions are protracted when compared to gas phase polymerization reactions performed via iCVD. For example, the gas phase polymerization of polytetrafluoroethylene (PTFE) via iCVD has deposition rates  $>100$  nm/min.<sup>3</sup> Such gas phase reactions have an advantage over surface reactions (with respect to deposition rate) that lack three-dimensional freedom for polymer chain and cross-link formation during the reaction. These complexities affect the deposition rate negatively, and the iCVD polymerization of V<sub>3</sub>D<sub>3</sub> is therefore relatively slow, ranging from 7–10 nm/min compared to 40–100 nm/min in a typical iCVD process.<sup>4,5</sup> This slow production rate of polyV<sub>3</sub>D<sub>3</sub> creates a large gap between laboratory synthesis and process scale-up to manufacturing standards. One way to overcome this problem is to introduce linear siloxane spacer molecules that have excess vinyl groups to increase the probability of interactions between the vinyl moieties of the siloxane pendant groups, produce a large number of cross-links, and thereby increase deposition rates.

In this article, we describe the synthesis of a novel copolymer of polyV<sub>3</sub>D<sub>3</sub> using V<sub>3</sub>D<sub>3</sub> as the monomer, TBP as the initiator, and hexavinylidisiloxane (HVDS) as the spacer. An array of heated constantan filament wires is used to generate primary peroxide radicals and initiate polymerization. The reaction is found to be initiator dependent with deposition rates ranging from 18 to 30 nm/min. Because of the presence of six functional vinyl groups on the spacer and three on the monomer, the resulting polymer is highly cross-linked, rendering it insoluble in common laboratory solvents. Furthermore, the copolymer is shown to have attractive electrical insulation characteristics.

## Experimental Section

**Sample Preparation.** Samples were prepared in a custom-built vacuum chamber (Sharon Vacuum) as described previously.<sup>6,7</sup> The cylindrical chamber has an outer diameter of 240 mm and a height of 33 mm. A 25 mm thick quartz plate was used to cover the reactor and also served as a view port, allowing visual inspection of the deposition process. Films were deposited on 100 mm diameter silicon wafers (Waferworld) that were rinsed with isopropyl alcohol and dried using nitrogen prior to deposition. 0.5 mm diameter

\* Corresponding author: Ph +1 (617) 373-4017; Fax +1 (617) 373-2209; e-mail smurthy@coe.neu.edu.

<sup>†</sup> Northeastern University.

<sup>‡</sup> GVD Corporation.

**Table 1. Reactor Conditions for the Deposition of iCVD PolyV<sub>3</sub>D<sub>3</sub>–HVDS Films**

sample name	reactor pressure (mTorr)	stage temperature (K)	filament temperature (K)	V <sub>3</sub> D <sub>3</sub> flow rate (sccm)	TBP flow rate (sccm)	HVDS flow rate (sccm)
A1	275	333	773	6	0.50	1
A2	275	333	773	6	0.75	1
A3	275	333	773	6	1.00	1
A4	275	333	773	6	1.25	1
A5	275	333	773	6	1.50	1
A6	275	333	773	6	1.75	1
B1	275	323	773	6	1.50	1
B2	275	328	773	6	1.50	1
B3	275	333	773	6	1.50	1
B4	275	338	773	6	1.50	1
B5	275	343	773	6	1.50	1
C1	275	333	648	6	1.50	1
C2	275	333	673	6	1.50	1
C3	275	333	698	6	1.50	1
C4	275	333	723	6	1.50	1
C5	275	333	748	6	1.50	1
C6	275	333	773	6	1.50	1

annealed constantan wires (55% Cu 45% Ni; Goodfellow) were used as filament wires and resistively heated using a variable ac power source. The filament wires were strung onto a stainless steel frame and placed 20 mm above the substrate. A thermocouple (Type K, AWG36, Omega Engineering) was directly attached to one of the filaments to monitor the filament temperature. The reactor pressure was controlled using a throttling butterfly valve (Intellisys, NorCal) connected to an autotuned digital controller (Intellisys, NorCal). The substrate temperature was maintained by the circulation of heated silicone oil on the backside of the reactor stage and measured by taping a thermocouple (Type K, AWG36, Omega Engineering) on the base of the cylindrical reactor.

The monomer (1,3,5-trivinyltrimethylcyclotrisiloxane, 99%; Silar Laboratories) and initiator (*tert*-butyl peroxide, 98%; Aldrich) were used as is without purification. The monomer was evaporated in a Pyrex jar maintained at  $85 \pm 2$  °C, and vapor flow was controlled by a mass flow controller (Model 1152; MKS). The initiator was maintained at  $40 \pm 2$  °C, and its flow was controlled by another mass flow controller (Model 1179A, MKS). The spacer (hexavinyldisiloxane, Gelest) was maintained at  $90 \pm 2$  °C, and its flow rate was controlled through a manually operated needle valve. The precursor vapors were fed to the reactor via a distribution plate to ensure uniform flow distribution. Film depositions were monitored using an in situ interferometry system equipped with a 633 nm laser source (JDS Uniphase). To calculate the order of the polymerization reaction and to obtain the infrared spectra of polyV<sub>3</sub>D<sub>3</sub>, three separate sets of conditions were utilized following previous work from O'Shaughnessy et al.<sup>1</sup> All samples were baked at 250 °C for 90 min postdeposition in a vacuum oven to remove unreacted monomer and other adsorbed impurities.

**Film Characterization.** Thickness measurements were conducted by using variable-angle spectroscopic ellipsometer (J.A. Woollam M-2000, xenon light source). A Cauchy–Urbach model was used to acquire a nonlinear least-squares fit of the data obtained at either one or three angles (68° or 65°, 70°, and 75°) and 225 wavelengths. Fourier transform infrared (FTIR) spectroscopy was carried out on a Nicolet Nexus 870 ESP spectrometer in normal transmission mode. A DTGS KBr detector was utilized over the range of 400–4000 cm<sup>−1</sup> with a 4 cm<sup>−1</sup> resolution. All measurements were averaged over 128 scans. All spectra were baseline corrected and thickness-normalized.

Resistance measurements were carried out using a Keithley 617 electrometer attached to the sample by adhesive electrodes (Tyco Healthcare). The electrometer reading was allowed to stabilize for 30 min, and sample resistivity was calculated by multiplying the measured resistance by the ratio of the electrode area by the sample thickness (determined by ellipsometry). Solubility testing was performed by immersing coated silicon substrates in tetrahydrofuran, acetone, isopropanol, and dimethyl sulfoxide (all obtained from Fisher Scientific) for 30 min, followed by drying with Dust-Off

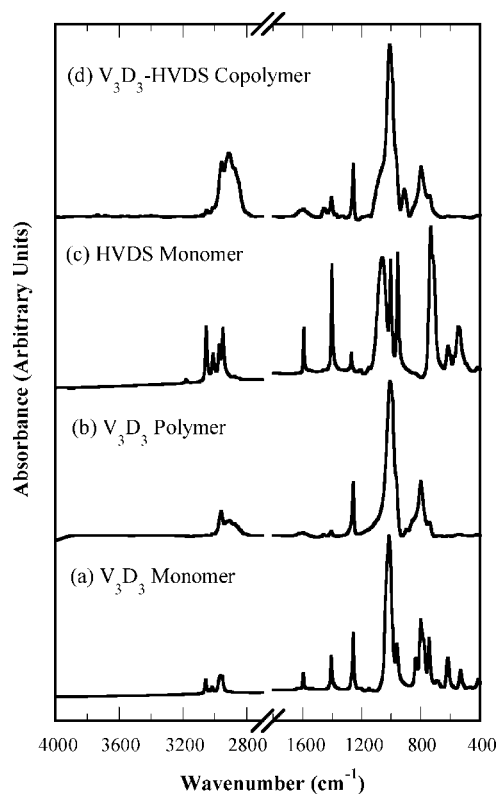


**Figure 1.** FTIR spectra of V<sub>3</sub>D<sub>3</sub> monomer, V<sub>3</sub>D<sub>3</sub> polymer, HVDS monomer, and V<sub>3</sub>D<sub>3</sub>–HVDS copolymer. The presence of absorption peak characteristic to the Si–O–Si ring structure at 1012 cm<sup>−1</sup> is evident in all V<sub>3</sub>D<sub>3</sub>-associated spectra.

(Falcon). Film thickness was measured by ellipsometry before and after immersion. Adhesion to silicon wafer substrates was quantified by using ASTM tape test D3359-02. 1 mm square grids were scored onto the sample, and an adhesive tape (P99 polyester tape; Pemacel) was applied and secured. The tape was then removed rapidly per ASTM guidelines and the sample visually inspected to assess film removal from the substrate. Adhesion tests were also performed before and after boiling coated silicon wafer samples in deionized water for 60 min.

## Results and Discussion

**Infrared Spectroscopy.** Reactor conditions were maintained following previous work by O'Shaughnessy et al.<sup>1,2</sup> Experiments were performed in three separate sets (A–C) as shown in Table 1 where subsets A, B, and C represent experiments with increasing initiator partial pressure, substrate temperature, and filament temperature, respectively. For the deposition of polyV<sub>3</sub>D<sub>3</sub>–HVDS copolymer films, condition A5 provided the highest deposition rate and best overall material properties (as described below) and thus was chosen as a reference for subsequent experiments. Figure 1a–d shows FTIR absorption spectra for the V<sub>3</sub>D<sub>3</sub> monomer, the V<sub>3</sub>D<sub>3</sub> polymer deposited following prior work,<sup>1,2</sup> the HVDS monomer, and the V<sub>3</sub>D<sub>3</sub>–HVDS copolymer deposited per condition A5, respectively. Table 2 provides a list of FTIR absorption frequencies and peak intensities.<sup>8–10</sup> The spectra from Figure 1b and Figure 1d for polyV<sub>3</sub>D<sub>3</sub> and polyV<sub>3</sub>D<sub>3</sub>–HVDS are similar but have some key differences. The strong Si–O–Si absorption at 1012 cm<sup>−1</sup> is characteristic of cyclotrisiloxanes and provides evidence for retention of the ring structure.<sup>11,12</sup> In the spectrum of polyV<sub>3</sub>D<sub>3</sub>–HVDS (Figure 1d), a shoulder (that is not present in polyV<sub>3</sub>D<sub>3</sub>) around 1080–1090 cm<sup>−1</sup> is seen which is representative of linear Si–O chains and provides evidence for the incorporation of spacer molecule. This linear siloxane peak

Table 2. Absorption Band Assignments for Infrared Spectra

group	iCVD polyV <sub>3</sub> D <sub>3</sub> -HVDS (cm <sup>-1</sup> )	literature (cm <sup>-1</sup> )	intensity	reference
Si-O-Si symmetric stretch	510	~500	weak	9
Si-CH=CH <sub>2</sub>	612	610	weak	10
Si-C stretching, CH <sub>3</sub> rocking in Si-Me <sub>2</sub>	805	805	medium	9
Si-C stretching, CH <sub>3</sub> rocking in Si-Me <sub>3</sub>	837	845	strong	9
=CH <sub>2</sub> wag	920	950	medium	10
Si-O-Si asymmetric stretch	1012	1010–1020	strong	8
Si-O-Si (open chain)	1085–1090	1076–1093	weak	8
Si-CH <sub>3</sub> symmetric stretch	1260	1255–1280	strong	8
Si-CH <sub>2</sub> deformation	1408	1390–1410	medium	8
O-CH <sub>2</sub> deformation	1456	1445–1475	medium	8
C=C stretch vinylbond	1591	1590–1615	weak	8
CH <sub>3</sub> symmetric stretch	2873	2862–2882	medium	8
CH <sub>2</sub> asymmetric stretch	2911	2916–2936	strong	8
CH <sub>3</sub> asymmetric stretch	2958	2952–2972	strong	8
CH stretch vinyl group	3010	2995–3020	very weak	8
CH <sub>2</sub> symmetric stretch vinyl group	3050	3075–3090	weak	8

at 1080 cm<sup>-1</sup> also appears in thermally ring-opened cyclic siloxanes.<sup>1,13</sup> However, since all the polyV<sub>3</sub>D<sub>3</sub>-HVDS films were deposited at filament temperatures below 600 °C, polymerization via ring-opening is not likely. Furthermore, if the polymerization reaction had occurred via thermal ring-opening, the peak intensity at 1012 cm<sup>-1</sup> (characteristic of trifunctional cyclic siloxanes) compared to that of pure polyV<sub>3</sub>D<sub>3</sub> should have reduced intensity as shown by O'Shaughnessy et al.<sup>1</sup> When the spectra for polyV<sub>3</sub>D<sub>3</sub> and polyV<sub>3</sub>D<sub>3</sub>-HVDS are compared as shown in Figure 1b,d, the peak intensity shows no apparent reduction and confirms the incorporation of spacer as opposed to polymerization via ring opening. Moreover, there exists an additional strong peak at 2911 cm<sup>-1</sup> in Figure 1d compared to that of polyV<sub>3</sub>D<sub>3</sub> in Figure 1b, which is representative of the CH<sub>2</sub> asymmetric stretching mode and further substantiates the incorporation of spacer molecule into the film of polyV<sub>3</sub>D<sub>3</sub>-HVDS.

Figure 2 shows the FTIR spectra of the films deposited with increasing TBP partial pressures of 14, 32, and 50 mTorr (conditions A1, A3, and A5, respectively, in Table 1). At first glance, all of the spectra in Figure 2 appear nearly identical. The spectrum shown in Figure 2a looks similar to that of polyV<sub>3</sub>D<sub>3</sub> in Figure 1b but consists of a very small shoulder near 1080 cm<sup>-1</sup> (representing Si-O bonding in linear siloxane molecules<sup>8</sup>). This shoulder is small compared to that in the spectra shown in Figure 2b,c. Additionally, Figure 2a shows only a slight increase in the 2911 cm<sup>-1</sup> peak associated with CH<sub>2</sub> asymmetric stretching mode compared to Figure 1b, showing that at lower partial pressures of TBP spacer incorporation, although present, is relatively minor. Figure 3a–c is an enlargement of Figure 2 where the spectral region 900–1500 cm<sup>-1</sup> is shown for the purpose of clarity. In contrast to the spectrum shown in Figure 3a, the spectra in Figure 3b,c have a shoulder at 1080 cm<sup>-1</sup> that is relatively more conspicuous. The reason for the greater prominence of this shoulder lies in the fact that with higher TBP partial pressures more spacer is incorporated into the film. As a result, the peak intensity for long open chain siloxanes at 1080 cm<sup>-1</sup> increases gradually as shown in Figure 3b,c. This fact is further substantiated when the peak associated with the O-CH<sub>2</sub> deformation mode at 1456 cm<sup>-1</sup> is examined in Figure 3b,c. This peak is relatively more prominent in the films deposited at higher TBP partial pressures as seen in Figure 3b,c, indicating the incorporation of additional spacer at those conditions.

Another attribute to notice in Figure 2a–c is the reduction in peak intensities associated with Si-CH=CH<sub>2</sub> at 620 cm<sup>-1</sup>, the Si-CH<sub>2</sub> deformation mode at 1408 cm<sup>-1</sup>, and the C=C stretching mode of vinyl groups at 1591 cm<sup>-1</sup>, compared to the V<sub>3</sub>D<sub>3</sub> and HVDS monomer spectra in Figure 1a,c. Additionally,

the HVDS monomer spectrum shown in Figure 1c possesses two strong peaks near 740 cm<sup>-1</sup> and other at 955 cm<sup>-1</sup> which are likely be associated with CH<sub>2</sub> wagging modes in vinyl groups as reported by Rau and Kulisch.<sup>10</sup> Both of these peaks are also shown to drastically diminish in intensity in all the three polyV<sub>3</sub>D<sub>3</sub>-HVDS spectra shown in Figure 2a–c. All of the above attenuations in peak intensities suggest that the vinyl moiety in the polyV<sub>3</sub>D<sub>3</sub>-HVDS film is present in minute quantities. Another important peak to be noticed in all the three spectra shown in Figure 2a–c is the peak associated with Si-CH<sub>3</sub> symmetric stretching mode at 1260 cm<sup>-1</sup>. This peak remains unaltered by the change in TBP partial pressure, indicating that the CH<sub>3</sub> group bonded to the Si unit of the V<sub>3</sub>D<sub>3</sub> monomer is not involved in the entire polymerization reaction. The presence of very few vinyl moieties in the polymer film and the nonreactive nature of the CH<sub>3</sub> moiety bonded to Si atom

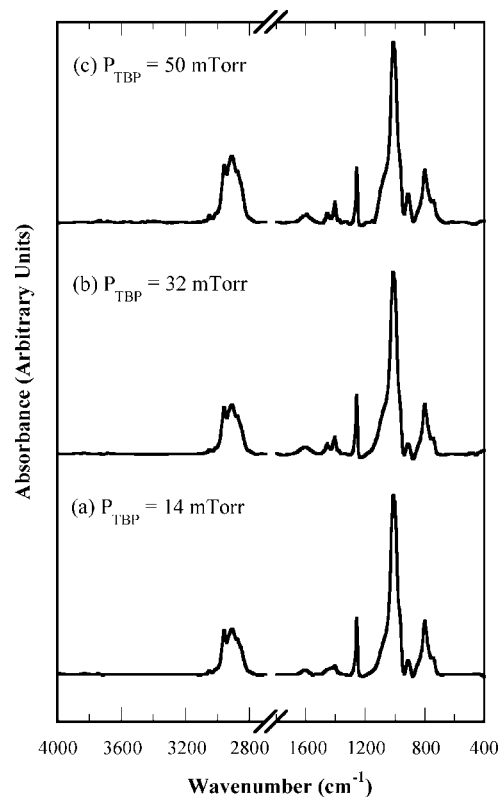
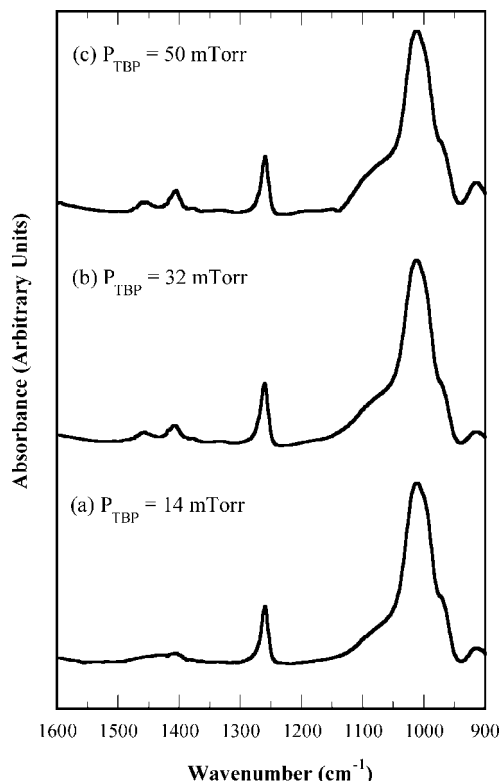


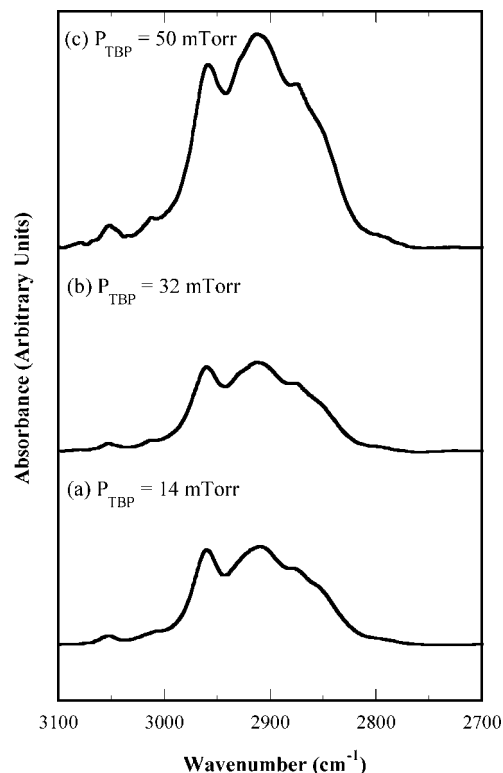
Figure 2. FTIR spectra of films deposited at varying partial pressures of initiator (conditions A1, A3, and A5 in Table 1). (a), (b), and (c) represent films deposited at partial pressures 14, 32, and 50 mTorr, respectively.



**Figure 3.** Enlargement of the 900–1500  $\text{cm}^{-1}$  region of the FTIR spectra shown in Figure 2. The increase in intensity of the 1080  $\text{cm}^{-1}$  peak in (b, c) compared to (a) indicates incorporation of linear Si–O–Si chains. Additionally, there is an increase in the intensity of the 1456  $\text{cm}^{-1}$  peak (corresponding to O–CH<sub>2</sub> deformation mode) in (b, c) that further corroborates the incorporation of spacer.

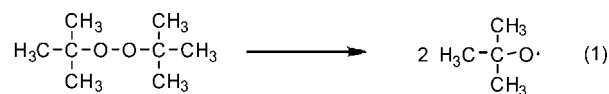
leads to the hypothesis that the polymerization reaction occurs through the vinyl groups of V<sub>3</sub>D<sub>3</sub> and HVDS, similar to the observation of O'Shaughnessy et al.<sup>1</sup> for polyV<sub>3</sub>D<sub>3</sub> films.

Figure 4 is an enlargement of a segment of Figure 2 that emphasizes the absorption peaks ranging from 2700 to 3100  $\text{cm}^{-1}$ . This enlarged view provides vital information about the changes in relative intensities of absorption peaks related to (CH)<sub>x</sub> groups in unsaturated and saturated carbons of polyV<sub>3</sub>D<sub>3</sub>–HVDS with increasing TBP partial pressures. From Figure 4c, it is evident that as the TBP partial pressure is increased, the 2911  $\text{cm}^{-1}$  and the 2958  $\text{cm}^{-1}$  peak intensities increase. The former is not surprising considering the fact that HVDS has six vinyl groups which, when polymerized, give rise to saturated –CH<sub>2</sub>– groups. Hence, higher TBP partial pressures result in more initiated chains, giving rise to an increase in repeated –CH<sub>2</sub> units in addition to TBP-terminated groups. Since these terminated groups possess –CH<sub>3</sub> moieties, the intensity of 2958  $\text{cm}^{-1}$  peak also increases as the TBP partial pressure is increased. The fact that increasing TBP partial pressure results in an increase in (–CH<sub>2</sub>–CH<sub>2</sub>–)<sub>n</sub> units indicates that at higher TBP partial pressures, the relative amount of the polyethylene chains increase due to spacer incorporation. Further evidence comes from examining absorption peaks above 3000  $\text{cm}^{-1}$ . Absorptions above 3000  $\text{cm}^{-1}$  are known to be related to C–H bonds in unsaturated carbons,<sup>8</sup> and these are abundant in HVDS monomer shown in Figure 1. Since both of the strong peaks in Figure 4a–c, i.e., the CH<sub>2</sub> asymmetric stretching mode at 2911  $\text{cm}^{-1}$  and the CH<sub>3</sub> asymmetric stretching mode at 2958  $\text{cm}^{-1}$ , are below 3000  $\text{cm}^{-1}$ , it can be hypothesized that the majority of the double bonded C–H groups corresponding to vinyl moieties are saturated during the polymerization reaction. Moreover, all the peaks related to C–H bonds in unsaturated carbons are greatly reduced when compared to the spectrum of



**Figure 4.** Enlargement of the 2700–3100  $\text{cm}^{-1}$  region of the FTIR spectra shown in Figure 2. Note the increase in intensity of the 2911  $\text{cm}^{-1}$  peak proving incorporation of saturated CH<sub>2</sub> chains due to the integration of spacer molecules into the film.

**Scheme 1**



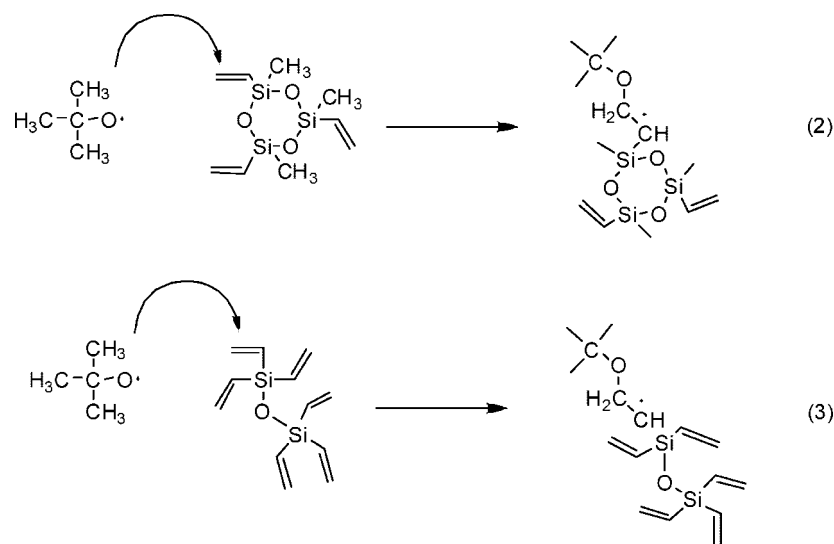
V<sub>3</sub>D<sub>3</sub> and HVDS monomer in Figure 1, again confirming the incorporation of polyethylene chains as the TBP partial pressure is increased.

Inspection of the spectra shown in Figures 2c and 4c provides insights into the effect of increase in initiator partial pressures on the unreacted vinyl groups present in the polyV<sub>3</sub>D<sub>3</sub>–HVDS films deposited at condition A5. A key consequence of increasing the TBP partial pressure is that more spacer is incorporated into the film, which leaves more vinyl groups available for polymerization. Not all of these vinyl groups can undergo reaction due to steric hindrance and lack of initiator contact. The unreacted vinyl groups are manifested by the small increase in the intensity of peaks associated with =CH<sub>2</sub> wagging mode (920  $\text{cm}^{-1}$ ), C=C stretch (1591  $\text{cm}^{-1}$ ), and the CH<sub>2</sub> symmetric stretch (3050  $\text{cm}^{-1}$ ) in Figures 2c and 3c.

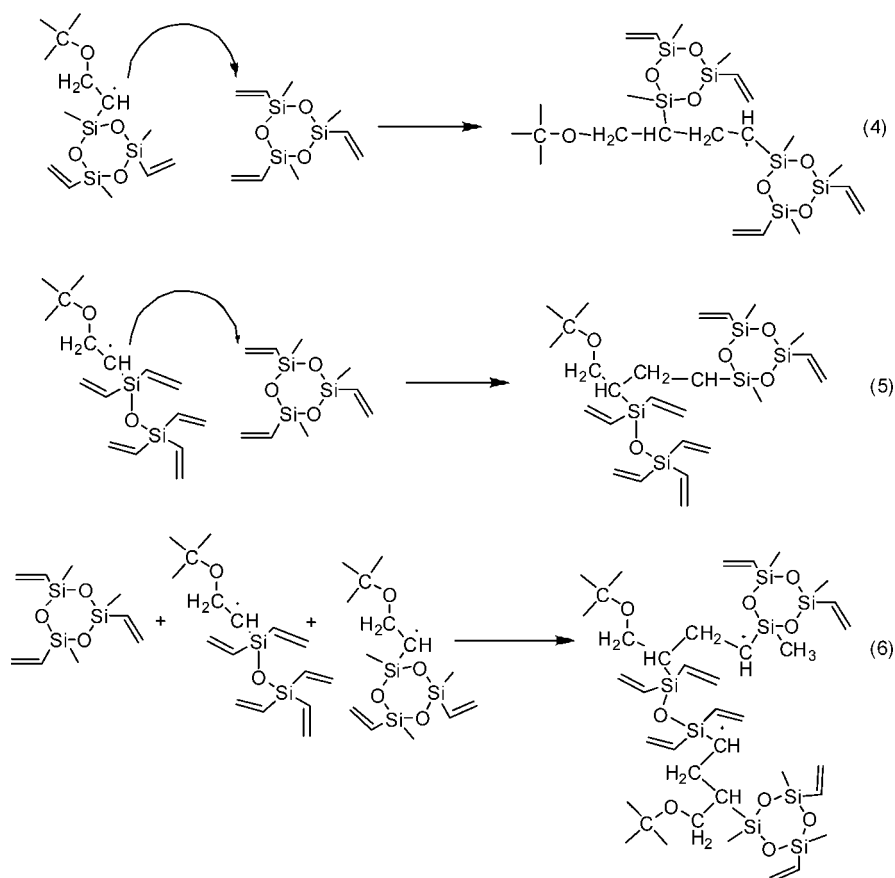
**Polymerization Mechanism.** The mechanism for the polymerization of polyV<sub>3</sub>D<sub>3</sub>–HVDS is hypothesized to consist of three steps, as shown in Schemes 1–3. The first step is the decomposition of initiator molecules into reactive radicals, as illustrated in Scheme 1. The formation of TBP radicals in iCVD polymerization is known to occur at filament temperatures of 200–250 °C<sup>1,6,14</sup> via the cleavage of the O–O bond.<sup>15</sup> These radicals react with the vinyl groups present on the V<sub>3</sub>D<sub>3</sub> and HVDS monomer molecules to initiate chain growth, as shown in Scheme 2. The subsequent addition of monomer units to the chains is shown in Scheme 3. The initiation and chain growth reactions result in the conversion of vinyl moieties into (–CH<sub>2</sub>–)<sub>n</sub> groups as evidenced by the FTIR spectra in Figure 2a–c where the peak intensities associated with Si–CH=CH<sub>2</sub>



Scheme 2



Scheme 3



at  $620\text{ cm}^{-1}$ , C=C stretching mode at  $1591\text{ cm}^{-1}$ , Si-CH<sub>2</sub> deformation mode at  $1408\text{ cm}^{-1}$ , and the  $720\text{ cm}^{-1}$  peak associated with CH<sub>2</sub> wagging mode are all greatly reduced compared to those in the V<sub>3</sub>D<sub>3</sub> and HVDS monomer spectra in Figure 1. Further evidence of chain growth via polymerization of vinyl groups is observed in Figure 4a–c where the peaks associated with the C–H stretching mode at  $3010\text{ cm}^{-1}$  and the CH<sub>2</sub> symmetric stretching mode at  $3050\text{ cm}^{-1}$  have reduced intensities relative to the V<sub>3</sub>D<sub>3</sub> and HVDS monomers.

Following activation of the V<sub>3</sub>D<sub>3</sub> and HVDS monomer molecules by the peroxide radicals, the side chains of V<sub>3</sub>D<sub>3</sub> monomer molecules grow by the addition of a secondary carbon

radical to unreacted vinyl moieties and by the successive addition of activated linear Si–O–Si hydrocarbons from HVDS. These linear Si–O–Si hydrocarbons can act as a bridge between any six-membered siloxane rings in the growing films and hence behave as a spacer as shown in Scheme 3 (eq 6). Since both the V<sub>3</sub>D<sub>3</sub> and HVDS monomers possess vinyl moieties, both can be activated by the initiator and grow independently. However, since HVDS possesses six vinyl groups, the probability of growing HVDS chains to readily find a tether point on a growing side chain of polyV<sub>3</sub>D<sub>3</sub> would be high. Hence, the postulated film structure is a network of polyV<sub>3</sub>D<sub>3</sub> chains with extensive cross-linking via linear poly(HVDS) chains. This

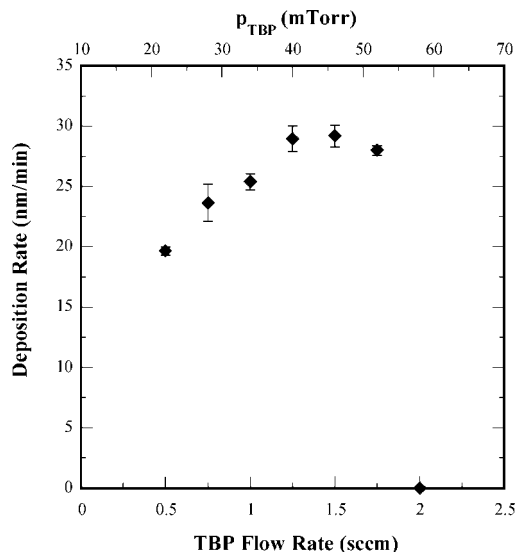


**Figure 5.** Deposition rate plotted as a function of partial pressure of TBP (A1–A6). Note the last data point at  $\sim 60$  mTorr which indicates a zero deposition rate.

hypothesis is supported by the fact that most of the poly $\text{V}_3\text{D}_3$ –HVDS films discussed earlier possess the ring structure in addition to substantial spacer incorporation.

The final step of the polymerization reaction would be chain termination, which might occur due to reactions between two growing chains or by end-capping with an activated peroxide radical.<sup>15</sup>

**Deposition Kinetics.** Figure 5 shows a plot of deposition rate as a function of TBP partial pressures (conditions A1–A6). The polymerization rate is more sensitive to changes in initiator partial pressures from 15 to 40 mTorr and appears to fall exponentially above 45 mTorr. Within this range (15–40 mTorr TBP), the rate is observed to be linear with respect to initiator concentration, suggesting that the polymerization of poly $\text{V}_3\text{D}_3$ –HVDS is a non-zero-order reaction with respect to the initiator. In the latter part of the curve in Figure 5, the deposition rate drops exponentially for initiator partial pressures of 45–50 mTorr. This drop-off can be attributed to either the formation of low molecular weight chains that are initiated and rapidly terminated (due an excess of activated TBP radicals) followed by desorption due to their high volatility or due to the higher recombination rate of the dissociated TBP at higher partial pressures.

To establish a basis for comparison with poly $\text{V}_3\text{D}_3$ –HVDS, three separate experiments were carried out to determine the reaction order for the polymerization of  $\text{V}_3\text{D}_3$ . These three experiments were carried out with constant monomer partial pressures and varying TBP partial pressures of 14, 32, and 50 mTorr. The film deposition rate remained essentially constant for all the three runs approximately  $7 \pm 2$  nm/min (detailed results not shown). Consequently, it was concluded that the reaction order for the polymerization with respect to initiator concentration of poly $\text{V}_3\text{D}_3$  was close to zero, in marked contrast with the nonzero order of polymerization of poly $\text{V}_3\text{D}_3$ –HVDS. The difference in reaction orders in the deposition of poly $\text{V}_3\text{D}_3$  and poly $\text{V}_3\text{D}_3$ –HVDS may be due to the presence of the spacer in the latter and hence requires relatively higher initiator concentrations to increase the deposition rate. Thus, it can be theorized that with the supply of sufficient initiator radicals each vinyl moiety in the spacer molecules becomes activated, and the spacer begins to incorporate into the film as the TBP concentration increases. Spectroscopic evidence shown in Figure 2a–c illustrates the incorporation of spacer into the film. Hence,

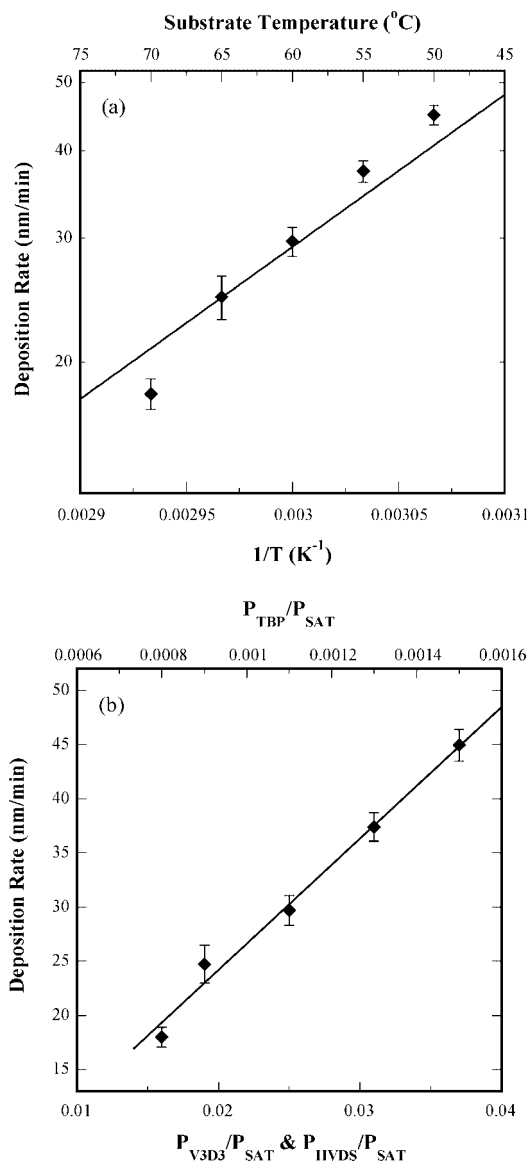


**Figure 6.** (a) Deposition rate as a function of substrate temperature. (b) Deposition rate as a function of  $P_{\text{V}_3\text{D}_3}/P_{\text{sat}}$  and  $P_{\text{HVDS}}/P_{\text{sat}}$  along with  $P_{\text{TBP}}/P_{\text{sat}}$  (B1–B5 in Table 1).

it is hypothesized that introducing HVDS results in enhanced interactions between any two large  $\text{V}_3\text{D}_3$  monomer molecules that are in close proximity, due to the presence of excess vinyl groups in the spacer. Furthermore, the incorporation of HVDS eliminates the need for the cyclic siloxane rings to align in certain conformations in order to form cross-links with neighboring chains. This relative reduction of steric hindrance is manifested as increasing deposition rate with rising initiator partial pressure (linear portion of the curve in Figure 5).

Figure 6a shows a semilog plot of deposition rate as a function of inverse substrate temperature (conditions B1–B5). Changing substrate temperature ( $T_{\text{sub}}$ ) would determine whether the concentration of the adsorbed species is a rate determinant or not. If the deposition rate increases with the decrease in  $T_{\text{sub}}$ , the concentration of the adsorbed species on the surface can be the rate-determining step.<sup>5</sup> On the other hand, if the initiation, propagation, and termination steps are rate-determining, the deposition rate should be improved by increasing the  $T_{\text{sub}}$ , since rate coefficients in such situations follow Arrhenius' law. Since the deposition conditions were maintained constant except for the  $T_{\text{sub}}$ , the only variable in the entire set of experiments, namely B1–B5 in Table 1, was the concentration of the adsorbed

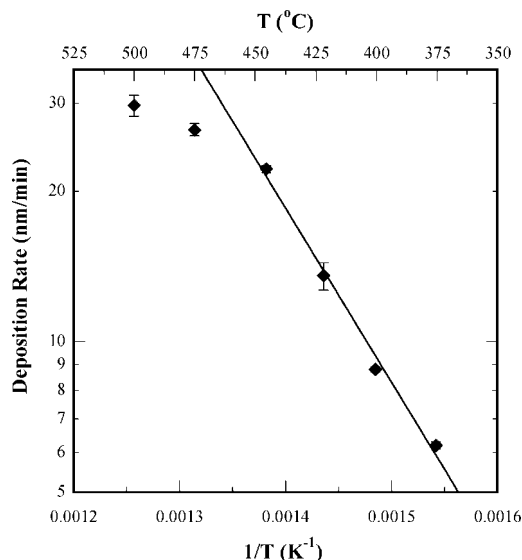


**Figure 7.** Deposition rate as a function of inverse filament temperature (C1–C6 in Table 1).

species on the surface. Standard adsorption isotherms such as the Brunauer–Emmett–Teller (BET) isotherm relate the ratio of monomer/spacer partial pressure to its saturation pressure ( $P_{V_3D_3}/P_{sat}$  and  $P_{HVDS}/P_{sat}$ ) qualitatively to the amount of adsorbed species.<sup>16</sup> Hence, to show the effect of adsorbed species on deposition rate, the values of  $T_{sub}$  in Figure 6a were transformed to  $P_{V_3D_3}/P_{sat}$  and  $P_{HVDS}/P_{sat}$  and plotted against deposition rate as shown in Figure 6b. The experiments B1–B5 were performed such that  $P_{V_3D_3}/P_{sat}$  and  $P_{HVDS}/P_{sat}$  had very close numerical values. The  $P_{sat}$  values for monomer, spacer, and the initiator were calculated using the Clausius–Clapeyron equation.<sup>17</sup>

Figure 6a shows that deposition rate increases as the  $T_{sub}$  decreases, reaching 46 nm/min at  $T_{sub} = 50$  °C. A linear curve fit provides a slope of 4993.2, corresponding to an apparent  $E_a$  value of  $-41.5$  kJ/mol. To understand the meaning of negative activation energy, a mathematical relationship between the concentrations of adsorbed species to  $T_{sub}$  is required. Recent work by Lau et al.<sup>4</sup> has shown that the concentration of adsorbed species on the surface is inversely proportional to the  $T_{sub}$  in a typical iCVD adsorption-limited system based on derivations starting from BET adsorption isotherms. But, the concentration of adsorbed species is directly related to the rate of reaction, and hence, the rate would be inversely proportional to  $T_{sub}$  for an adsorption-limited system. An inverse relationship of this type between deposition rates of polyV<sub>3</sub>D<sub>3</sub>–HVDS to  $T_{sub}$  is evident in Figure 6a where decrease in  $T_{sub}$  (or the increase in  $P_{AS}/P_{sat}$  in Figure 6b) results in a linear increase in deposition rate. Consequently, it can be concluded that the iCVD polymerization of polyV<sub>3</sub>D<sub>3</sub>–HVDS is predominantly controlled by the surface concentration of the adsorbed species and is therefore an adsorption-limited process.

Previous work by O'Shaughnessy et al.<sup>1</sup> has showed that thermal ring-opening of cyclic Si–O–Si chains of V<sub>3</sub>D<sub>3</sub> occurs above filament temperatures of 600 °C, and consequently, experiments in the present study were limited to a maximum filament temperature of 500 °C. Figure 7 shows a semilog plot of deposition rate as a function of inverse filament temperature for conditions C1–C6. The deposition rate is responsive to changes in filament temperature up to 450 °C and appears to plateau gradually at higher temperatures. The first four points in Figure 7 (right to left) can be considered to represent a kinetically limited regime. In this regime, the deposition rate is markedly receptive to changes in filament temperature. The latter part of the curve can be attributed to a transition from a kinetic

regime to a mass transport-limited regime as observed in many other chemical vapor deposition systems.<sup>1,12,17,18</sup> Figure 7 is an Arrhenius style plot usually used to calculate activation energy ( $E_a$ ) by fitting the data points to a linear curve.<sup>19</sup> However, such a calculation is not entirely justified in the current study because deposition rate is dependent on initiator concentration as shown in Figure 7. Nevertheless, keeping this in mind, the slope of the curve fit for the linear part of the curve was calculated to be  $-8022.2$ , corresponding to an estimated  $E_a = 66.7$  kJ/mol. The  $E_a$  necessary for breaking the O–O linkage in TBP radicals is known to be 108 kJ/mol.<sup>14</sup> Compared to this value, the  $E_a$  for the system in hand is much lower and provides essential information that initiator decomposition is not likely the rate-determining step. This again confirms the fact that the polymerization reaction is adsorption-limited and governed by the surface concentration of the adsorbed species.

Another important point to note is the difference in  $E_a$  values between the polymerization of polyV<sub>3</sub>D<sub>3</sub> ( $\sim 28$  kJ/mol)<sup>1</sup> and polyV<sub>3</sub>D<sub>3</sub>–HVDS (around 67 kJ/mol). This difference in  $E_a$  provides vital information about the polymerization mechanism. With the addition of the spacer molecules into the film, one might expect a reduction in  $E_a$  value that may result in an increase in polymerization rate. However, the apparent  $E_a$  value for the polymerization of polyV<sub>3</sub>D<sub>3</sub>–HVDS is higher than that of polyV<sub>3</sub>D<sub>3</sub>, suggestive of an elevated energy barrier and slower polymerization rate. Hence, it can be hypothesized that the increase in deposition rate for the polymerization of polyV<sub>3</sub>D<sub>3</sub>–HVDS may not be due to the reduction in energy barrier but rather a consequence of the presence of an additional reaction pathway where the chains of polymerized HVDS are able to readily find tether points in the main polymer chains and form cross-links. This hypothesis is corroborated by the arguments presented in the previous paragraphs where increasing TBP partial pressure results in incorporation of spacer and thus results in enhancement of the deposition rate.

**Physical Properties.** The bulk resistivity value of polyV<sub>3</sub>D<sub>3</sub>–HVDS film deposited at condition A5 is  $(5.6 \pm 1) \times 10^{14}$  Ω·cm and lies in between that of polyethylene ( $1 \times 10^{14}$  Ω·cm) and polyV<sub>3</sub>D<sub>3</sub> ( $(4.0 \pm 2) \times 10^{15}$  ohm·cm).<sup>21,2</sup> This is not surprising considering the fact that HVDS possesses six vinyl groups, and thus, the resistivity values are lower relative to polyV<sub>3</sub>D<sub>3</sub> due to the presence of additional linear polyethylene side chains. Although the bulk resistivity value for polyV<sub>3</sub>D<sub>3</sub>–HVDS is an order of magnitude lower than that of polyV<sub>3</sub>D<sub>3</sub>, the current insulating coating utilized for neural implants, parylene-C, has a bulk resistivity only slightly higher than that of polyV<sub>3</sub>D<sub>3</sub>–HVDS ( $1 \times 10^{15}$  Ω·cm).<sup>22</sup>

The adhesion of polyV<sub>3</sub>D<sub>3</sub>–HVDS films to silicon wafer substrates was assessed utilizing the ASTM D3359-02 tape test. Samples A1, A3, and A5 obtained a score of 5B corresponding to 0% delamination, the best possible score achievable by this test. Adhesion to silicon substrates is vital considering the long-term stability of the coating to the implanted neural probe because delamination of these coatings will result in various types of corrosion and finally lead to malfunction of the device.<sup>20</sup> Also, adhesion to substrates following contact with several solvents is important since the biological milieu possesses numerous components that might degrade these films after coming in contact with it.<sup>21</sup> Hence, adhesion tests were performed before and after soaking the samples in four different solvents, namely tetrahydrofuran, acetone, isopropyl alcohol, and dimethyl sulfoxide, for 30 min.

Table 3 shows solubility data at condition A5 for an array of common laboratory solvents. Adhesion test results are shown in the last column in Table 3 where all the samples were subjected to tape test without soaking and with soaking in conventional laboratory solvents. All of the samples obtained a

**Table 3. Film Thickness Measurements before and after Immersion in Solvents**

solvent	initial thickness (nm)	final thickness (nm)	adhesion rating before and after soak
tetrahydrofuran	130.6 ± 1.6	126.4 ± 4.3	5B (0% removal)
acetone	139.7 ± 1.5	141.9 ± 1.3	5B (0% removal)
isopropyl alcohol	137.7 ± 1.5	135.1 ± 1.4	5B (0% removal)
dimethyl sulfoxide	130.7 ± 4.5	135.8 ± 4.5	5B (0% removal)

score of 5B indicating 100% film retention, and no loss of coating was observable before and after soaking. Enduring coatings for polar solvents are largely preferred for permanently implantable materials. When Table 3 is examined, there is no loss of thickness in films in either polar or nonpolar solvents, clearly representative of insoluble behavior of polyV<sub>3</sub>D<sub>3</sub>-HVDS. This is likely a consequence of polyV<sub>3</sub>D<sub>3</sub>-HVDS being an extremely cross-linked polymer that possesses no low molecular weight chains, as indicated by the FTIR data in Figure 1. (If the films had short Si-O-Si side chains, there should have been new absorption peaks located at either 1135 or 1190 cm<sup>-1</sup>.<sup>8</sup>) None of the films show absorption peaks at these wavenumbers, and none of the films are soluble in any of the aforementioned solvents. The only exception occurs when polyV<sub>3</sub>D<sub>3</sub>-HVDS films are deposited at  $T_{\text{sub}} < 55$  °C. For depositions below 55 °C, upon reactor pump up to atmospheric pressure, the films possess small visible islands of disk-shaped voids mainly due to the desorption of entrained molecules or short chain oligomers formed during deposition. These small molecules or short side chains also imply that the resulting deposited polymer is not sufficiently cross-linked and hence would serve as an indirect qualitative method to screen out uncross-linked polyV<sub>3</sub>D<sub>3</sub>-HVDS films. When these kinds of low molecular weight molecules are present, the films become sparingly soluble in all the solvents mentioned above (results not shown). This phenomenon underscores the importance of maintaining higher  $T_{\text{sub}}$  values although deposition rate drops at higher  $T_{\text{sub}}$  values as shown earlier. Maintaining higher  $T_{\text{sub}}$  also decreases the probability of forming smaller side chains that help to keep the films intact without dissolving in common solvents.

Figure 8 shows the FTIR spectra of polyV<sub>3</sub>D<sub>3</sub>-HVDS films deposited at condition A5 and subjected to a boiling water test. Figure 8a represents the spectrum of the film as deposited, and Figure 8b corresponds to a film that was boiled in DI water for 60 min at atmospheric pressure. There are no visible changes in the spectra after boiling, signifying the hydrolytic stability of the film. This means that there are no hydrolytically labile groups in the film which could alter the film chemical structure in the rigorous aqueous environment. Additionally, adhesion tests performed before and after boiling yielded a rating of 5B further showing stability of the coating. Moreover, if there were any change in chemical structure, new absorptions should have been observed between both 3400–3600 and 1000–1100 cm<sup>-1</sup> as seen in V<sub>3</sub>D<sub>3</sub>-H<sub>2</sub>O copolymer films described previously for the deposition of V<sub>3</sub>D<sub>3</sub> polymer films using water as a porogen to obtain low- $k$  materials via pulsed-plasma CVD.<sup>11</sup> Since polyV<sub>3</sub>D<sub>3</sub>-HVDS is a copolymer of polyethylene and polyV<sub>3</sub>D<sub>3</sub>, the fact that it is quite stable and inert to aqueous/saline milieu is not unforeseen.

## Conclusions

A novel polymer polyV<sub>3</sub>D<sub>3</sub>-HVDS has been synthesized by iCVD using V<sub>3</sub>D<sub>3</sub> as a monomer, HVDS as spacer, and TBP as initiator. Spectroscopic evidence shows that this polymer possesses cyclic siloxane rings as pendant groups and long polyethylene-siloxane side chains connected to other cyclic siloxane rings. The degree of spacer incorporation is directly

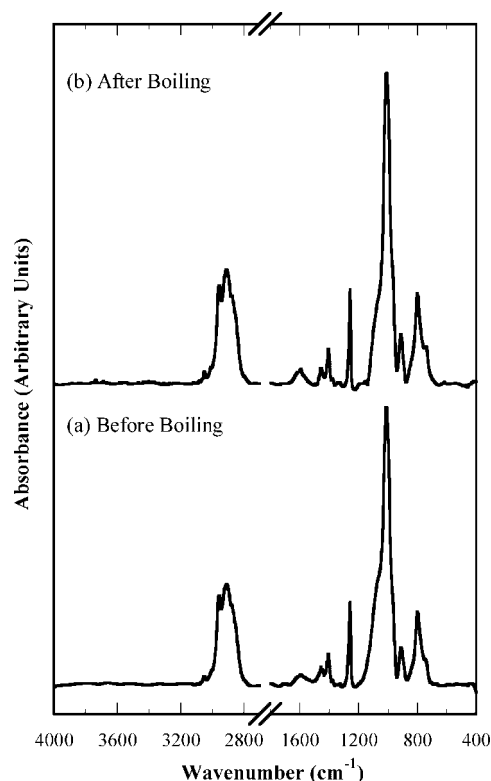


**Figure 8.** FTIR spectra of films deposited per condition A5 in Table 1: (a) as deposited and (b) following boiling in DI water for 60 min. Adhesion test before and after boiling yielded a rating of 5B (no delamination).

dependent on the concentration of the initiator. Almost 90% of the vinyl groups present in both the monomer and the spacer are reacted. The polymerization occurs via successive addition of initiated radicals of monomer and the spacer followed by chain growth and termination. The polymerization reaction is dependent on the concentration of the initiator and has enhanced deposition rates of ~30 nm/min at higher initiator concentrations. This is nearly a 4-fold increase when compared to polymerization of polyV<sub>3</sub>D<sub>3</sub> and quite amenable for a manufacturing process unit. The kinetics of polymerization is shown to be dependent on the concentration of adsorbed species on the surface, indicating that the film growth process is adsorption limited. The  $E_a$  value with respect to filament temperature is higher than that of polyV<sub>3</sub>D<sub>3</sub>, showing that the polymerization reaction is greatly affected by the decrease in steric barriers rather than  $E_a$  value.

The bulk resistivity of the polyV<sub>3</sub>D<sub>3</sub>-HVDS copolymer is comparable to that of polyV<sub>3</sub>D<sub>3</sub> and parylene-C. The films have excellent adhesion properties before and after soaking them in polar and nonpolar solvents. They are also hydrolytically stable and show no apparent change in their chemical structure after boiling in DI water for 1 h. The films are highly cross-linked and insoluble in ordinary laboratory solvents and have no low-molecular-weight chains that dissolve over time. Overall, the enhanced deposition rates of polyV<sub>3</sub>D<sub>3</sub>-HVDS indicate its potential to serve as an insulating coating for neural probes.

**Acknowledgment.** We gratefully acknowledge financial support from the National Institutes of Health through Grant R44 NS047952.

## References and Notes

- (1) O'Shaughnessy, W. S.; Gao, M. L.; Gleason, K. K. *Langmuir* **2006**, *22*, 7021.
- (2) O'Shaughnessy, W. S.; Murthy, S. K.; Edell, D. J.; Gleason, K. K. *Biomacromolecules* **2007**, *8*, 2564.



- (3) Lau, K. K. S.; Caulfield, J. A.; Gleason, K. K. *Chem. Mater.* **2000**, *12*, 3032.
- (4) Lau, K. K. S.; Gleason, K. K. *Macromolecules* **2006**, *39*, 3688.
- (5) Lau, K. K. S.; Gleason, K. K. *Macromolecules* **2006**, *39*, 3695.
- (6) Chan, K.; Gleason, K. K. *Chem. Vap. Deposition* **2005**, *11*, 437.
- (7) Chan, K.; Gleason, K. K. *Langmuir* **2005**, *21*, 8930.
- (8) Lin-Vien, D.; Colthup, N. B.; Fately, W. G.; Grasselli, J. C. In *The Handbook of Infrared and Raman Characteristic Frequencies of Organic Molecules*; Academic Press: San Diego, CA, 1991.
- (9) Lipp, E. D.; Smith, A. L. In *The Analytical Chemistry of Silicones*; Smith, A. L., Ed.; John Wiley & Sons: New York, 1991, p 305.
- (10) Rau, C.; Kulisch, W. *Thin Solid Films* **1994**, *249*, 28.
- (11) Burkey, D. D.; Gleason, K. K. *J. Appl. Phys.* **2003**, *93*, 5143.
- (12) Murthy, S. K.; Olsen, B. D.; Gleason, K. K. *Langmuir* **2002**, *18*, 6424.
- (13) Murthy, S. K.; Olsen, B. D.; Gleason, K. K. *J. Appl. Polym. Sci.* **2004**, *91*, 2176.
- (14) Mao, Y.; Gleason, K. K. *Langmuir* **2004**, *20*, 2484.
- (15) Odian, G. G. In *Principles of Polymerization*, 3rd ed.; Wiley: New York, 1991.
- (16) Adamson, A. W.; Gast, A. P. In *Physical Chemistry of Surfaces*, 6th ed.; John Wiley & Sons: New York, 1997.
- (17) Lewis, H. G. P.; Caulfield, J. A.; Gleason, K. K. *Langmuir* **2001**, *17*, 7652.
- (18) Pierson, O. H. In *Handbook of Chemical Vapor Deposition: Principles, Technology, and Applications*, 2nd ed.; Noyes Publications: Norwich, NY, 1999.
- (19) Fogler, H. S. In *Elements of Chemical Reaction Engineering*, 3rd ed.; Prentice Hall: Upper Saddle River, NJ, 1999.
- (20) Troyk, P. R.; Watson, M. J.; Poyezdala, J. J. *ACS Symp. Ser.* **1986**, *322*, 299.
- (21) Anderson, J. E.; Markovac, V.; Troyk, P. R. *IEEE Trans. Compon., Hybrids, Manuf. Technol.* **1988**, *11*, 152.
- (22) Mark, J. E. In *Polymer Data Handbook*, 3rd ed.; Oxford University Press: New York, 1999.

MA802330S